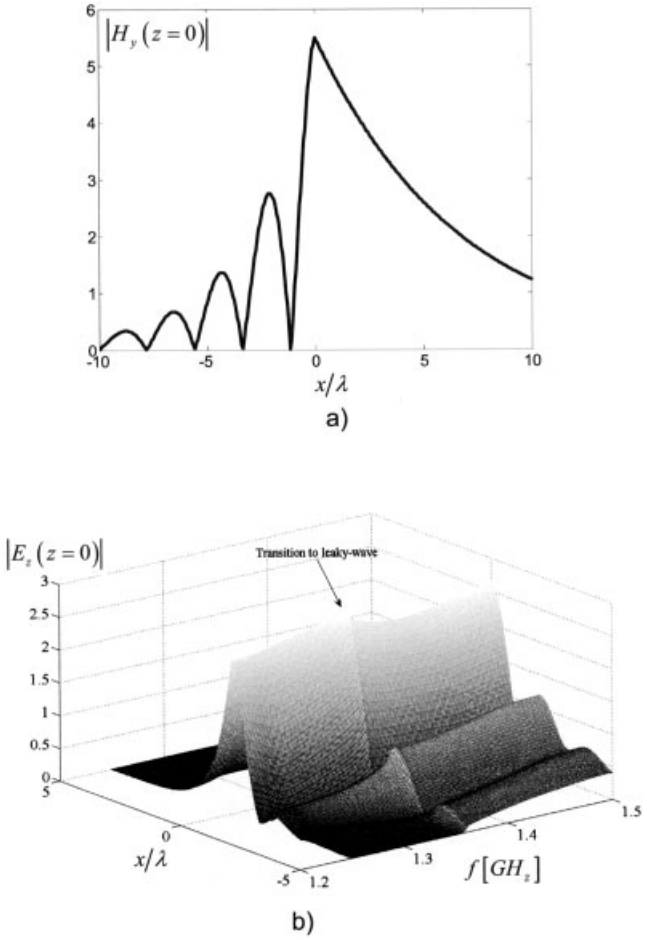

Figure 4 Electromagnetic field variation of surfaces and leaky modes: (a) 2D plot of the magnetic field H_y for $f = 0.65$ GH$_z$ in Region 1; (b) 3D plot of the electric field E_z in the frequency band of Region 2

isotropic media—namely, common isotropic or double-positive media from single-negative or double-negative media. These guided surface waves were also reported as possible solutions at isotropic–uniaxial and isotropic–biaxial interfaces. In this paper, we have shown that surface polaritons can also exist at an air–pseudochiral omega interface. Furthermore, we have also shown that proper leaky modes can occur at this special kind of isotropic–bianisotropic interface. Apart form its intrinsic significance and relevance, these new physical effects at isotropic–bianisotropic interfaces reveal that a thorough investigation of this type of planar interfaces can shed new light into the guidance and leakage properties of layered structures containing metamaterials, and other kinds of special materials, for microwave applications.

REFERENCES

1. R.E. Collin, Field theory of guided waves, 2nd ed., IEEE Press, Piscataway, New Jersey, 1991, pp. 697–704.
2. S.A. Tretyakov, Analytical modeling in applied electromagnetics, Artech House, Boston, 2003, pp. 233–236.
3. K. Welford, Surface plasmon-polaritons and their uses, Opt Quant Electron 23 (1991), 1–27.
4. A. Yariv and P. Yeh, Optical waves in crystals: Propagation and control of laser radiation, Wiley, New Jersey, 2003, pp. 489–495.
5. S.A. Tretyakov, I.S. Nefedov, C.R. Simovski, and S.I. Maslovski, Modelling and microwave properties of artificial materials with negative parameters, In: S. Zouhdi, A. Sihvola, and M. Arsalane (Eds.), Advances in electromagnetics of complex media and metamaterials, Kluwer Academic, Dordrecht, 2002, pp. 99–122.
6. M.I. D'Yakonov, New type of electromagnetic wave propagating at an interface, Sov Phys JETP 67 (1988), 714–716.
7. D.B. Walker, E.N. Glytsis, and T.K. Gaylord, Surface mode at isotropic-uniaxial and isotropic-biaxial interface, J Opt Soc Am A 15 (1998), 248–260.
8. H.C. Chen, Theory of electromagnetic waves: A coordinate-free approach, MacGraw-Hill, New York, 1983, pp. 299–339.
9. A. Serdyukov, I. Semchenko, S. Tretyakov, and A. Sihvola, Electromagnetics of bi-anisotropic materials: Theory and applications, Gordon and Breach, Amsterdam, 2001, pp. 15–43.
10. J.A. Kong, Maxwell equations, EMW Publishing, Cambridge, Massachusetts, 2002, p. 47.
11. M.M.I. Saadoun and N. Engheta, A reciprocal phase shifter using novel pseudochiral or Ω medium, Microwave Opt Technol Lett 5 (1992), 184–188.
12. M.M.I. Saadoun, The pseudochiral omega (Ω) medium: Theory and potential applications, Ph.D. Dissertation, University of Pennsylvania, September 1992.
13. A.L. Topa, C.R. Paiva, and A.M. Barbosa, Complete spectral representation for the electromagnetic field of planar multi-layered waveguides containing pseudochiral Ω-media, In: J.A. Kong (Ed.), Progress in electromagnetics research, PIER 18, EMW Publishing, Cambridge, Massachusetts, 1998, pp. 85–104.
14. A.L. Topa, C.R. Paiva, and A.M. Barbosa, Surface and leaky modes of multilayered omega structures, In: S. Zouhdi, A. Sihvola, and M. Arsalane (Eds.), Advances in electromagnetics of complex media and metamaterials, Kluwer Academic, Dordrecht, 2002, pp. 291–305.
15. A.L. Topa, C.R. Paiva, and A.M. Barbosa, Electromagnetic wave propagation in omega waveguides: Discrete complex modes and application to a ridge waveguide, In: J.A. Kong (Ed.), Progress in electromagnetics research, PIER 49, EMW Publishing, Cambridge, Massachusetts, 2004, pp. 309–331.

METAMATERIAL INCLUSIONS BASED ON GRID-GRAPH HAMILTONIAN PATHS

Vincenzo Pierro,[1] John McVay,[2] Vincenzo Galdi,[1] Ahmad Hoorfar,[2] Nader Engheta,[3] and Innocenzo M. Pinto[1]
[1] Department of Engineering
Waves Group
University of Sannio
I-82100, Benevento, Italy
[2] Department of Electrical and Computer Engineering
Villanova University
Villanova, PA 19085
[3] Department of Electrical and Systems Engineering
University of Pennsylvania
Philadelphia, PA 19104

Received 23 June 2006

ABSTRACT: *This article deals with a study of novel classes of metamaterial inclusions based on space-filling curves. The graph–theoretic Hamiltonian-path (HP) concept is exploited to construct a fairly broad class of space-filling curve geometries that include as special cases the well-known Hilbert an Peano curves whose application to metamaterial inclusions has recently been proposed. In this framework, the basic properties of HP are briefly reviewed, and a full-wave study of the electromagnetic properties of representative grid-graph HP geometries is carried out. Applications to metamaterial inclusions are explored, with focus on artificial magnetic conductors with reduced polarization-sensitivity.* © 2006 Wiley Periodicals, Inc. Microwave Opt Technol Lett 48: 2520–2524, 2006; Published online in Wiley InterScience (www.interscience.wiley.com). DOI 10.1002/mop.21982

Key words: *metamaterials; Hamiltonian paths; artificial magnetic conductors*

1. INTRODUCTION

During the past few years, there has been a growing interest in the use of wire structures based on space-filling curves [1] in a variety of electromagnetics (EM) engineering applications, including miniaturized antennas (see, Ref. 2–5), frequency selective surfaces [6], high-impedance surfaces [7, 8], double-negative metamaterials [9], and radio-frequency identification (RFID) [10]. In all the above applications, attention is principally focused on the most popular Hilbert and Peano [1] (pre-)fractal curves, whose space-filling and self-similarity properties are exploited to lower the frequency of operation (for a given spatial footprint) and to obtain multiband capabilities, respectively. However, the actual superiority of (pre-)fractal geometries, as compared to Euclidean space-filling curves, is still a controversial issue (see, Ref. 11–15).

Recently, we have been exploring the EM properties of an extended class of space-filling wire structures based on grid-graph (GG), Hamiltonian paths (HP), and cycles (HC) [16], which includes as special cases the Hilbert and Peano curves. Our studies are aimed at a better understanding of the basic relevant EM phenomena in *general* space-filling wire structures, their relation with local and global geometrical features, and the potential relevance and applications in the synthesis and/or optimization of novel devices/materials.

In this article, we exploit the GG-HP framework for generating more general and flexible classes of space-filling curves for metamaterial inclusions. After illustration of the basic properties of GG-HP geometries and their potentials, we focus on the computationally-affordable case of 6×6 GG-HC, for which we present a comprehensive full-wave study of the plane-wave scattering response. This study is aimed at revealing the wealth of EM responses attainable from this class of structures, as well as at identifying those configurations with potentially useful properties, such as predominant electric (or magnetic) polarizability, circularly-polarized response, reduced polarization-sensitivity, etc. Finally, we illustrate an application to artificial magnetic conductors.

2. GRID-GRAPH HAMILTONIAN PATHS IN A NUTSHELL

2.1. Some Definitions

For a better understanding of the basic properties of GG-HP geometries, a few definitions from graph theory are in order [17]. Given a *graph G*, i.e., an ordered couple (*V, E*) of a set of N *vertices* V and a finite set E of vertice-connecting *edges* (here assumed to be *undirected*), a *Hamiltonian path* (HP) in G is defined as a sequence $HP = (\nu_1,\nu_2,\ldots,\nu_N)$ such that: $\nu_i \varepsilon V$, $i = 1,\ldots,N$, $\nu_i \neq \nu_j$ for $i \neq j$, and $\{\nu_i,\nu_{i+1}\} \varepsilon E$, $i = 1,\ldots,N-1$ [18]. A closed HP ($\{\nu_N,\nu_1\} \varepsilon E$) is called a Hamiltonian *cycle* (HC) or *circuit*. In essence, a HP is characterized by visiting *all* the graph vertices *exactly once* [18]. This concept, first introduced in 1897 by Sir W. R. Hamilton as a *puzzle* ("icosian game"), has become a canonical problem in graph theory, with important recent applications in network routing and fault tolerance. Of particular interest in our investigation are HP in grid-graphs (GG), which have been studied extensively in the combinatorial computing literature [19].

The above graph-based *abstract* HP definition can readily be associated with space-filling curves via an intuitive *geometrical* representation of the graph vertices (points in a Euclidean space) and edges (connecting lines). For instance, by considering a rectangular $n \times m$ GG and its geometrical rectangular-lattice representation with edge-length L_e, HP can be associated to a family of space-filling curves, with the same total length $L_{HP} = (nm-1)L_e$ ($L_{HC} = nmL_e$ for cycles) and internal area $A_{HC} = (nm-2)L_e^2/2$, that pass through *all* the lattice vertices. Interestingly, this family contains as special cases the Hilbert ($2^k \times 2^k$ GG, for k-th iteration) and Peano ($3^k \times 3^k$ GG, for k-th iteration) curves. For instance, Figure 1 shows some HP realizations in a 2×2 GG. The realization in Figure 1(a) is readily recognized to be the 2nd-iteration of a Hilbert curve [1]. The other curves are examples of HP having the same endpoints as the Hilbert curve [Figs. 1(b) and 1(c)], different endpoints [Fig. 1(d)], or *coincident* endpoints [HC, Figs. 1(e) and 1(f)].

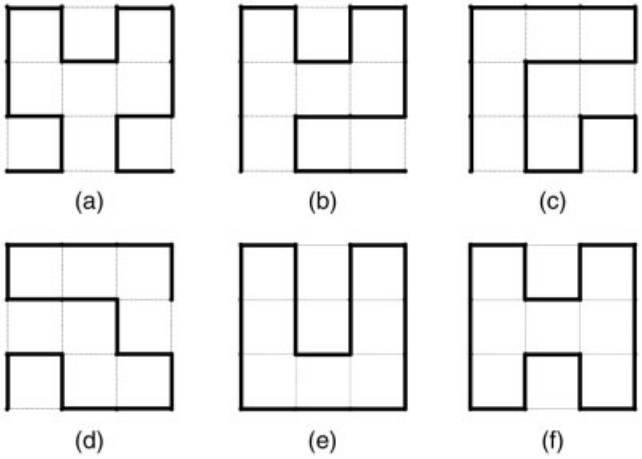

Figure 1 Examples of HP and HC realizations in a 4×4 GG. (a) Hilbert curve (2nd-iteration); (b), (c) HP with same endpoints as Hilbert; (d) HP with different endpoints; (e), (f) HC

2.2. Algorithmic Aspects

From the algorithmic viewpoint, the HP generation is known to be an *NP-complete* problem (hardest class in complexity theory) [20], generally not solvable in polynomial time for most graph classes (including GG). Even the *a priori* enumeration problem is very hard, and can be addressed analytically only for few classes. For instance, HC can be proved to exist in $n \times m$ GG provided n or m are even, and their enumeration [21] reveals a growth *faster than exponential* with the graph size (e.g., 6 in 4×4 GG, 1072 in 6×6 GG, 4,638,576 in 8×8 GG).

Typical HP generation algorithms can be divided into two main categories: (i) Backtrack-type (see, Ref. 22, 23), based on recursive search for all potential solutions (using some kind of pruning to restrict the search) and (ii) heuristic algorithms (see, Ref. 24), based on simplifying assumptions (local search, randomization, etc.). Backtrack-type algorithms are capable of finding *all* possible solutions, at the expense of *longer* computing times (scaling exponentially, in the worst case). Heuristic algorithms tend to be significantly *faster* (linear or low-order polynomial time), but may *not* find all solutions.

In our investigation, we used a slightly different approach, based on the equivalence between the HP search problem and the celebrated Traveling Salesman Problem (TSP) [25]. Intuitively, finding HP in a given graph can be recast into a TSP on a "weighted" graph, where one assigns a "cost" to each possible edge and solves an optimization problem aimed at finding the "cheapest" path, for which well-established computational engines [e.g., Concorde (http://www.tsp.gatech.edu/concorde.html)] are available. In this framework, for an assigned graph topology (parameterized, e.g., via the adjacency matrix [17]), admitted

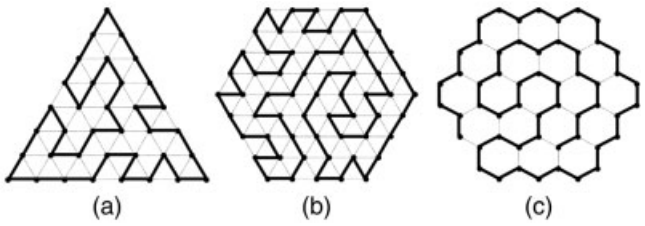

Figure 2 Examples of HP and HC realizations in non-Cartesian lattices with non-rectangular footprints. (a) HC in triangular lattice with triangular footprint; (b) HC in triangular lattice with hexagonal footprint; (c) HP in hexagonal lattice with hexagonal footprint

edges (i.e., those connecting *adjacent* vertices) are assigned a *low* cost, whereas non-admitted edges are assigned a *very high* cost (so as to be always disregarded in the optimization procedure). This approach is very powerful and flexible, and quite easy to implement. In particular, it also allows the generation of *constrained* realizations, via the assignment of particularly low costs to certain of the admitted edges, thereby favoring their appearance (see the examples discussed below).

2.3. Hamiltonian Paths vs. Hilbert/Peano Curves

From the above elements, it appears suggestive to utilize the HP framework for generation and exploration of rather *general* classes of space-filling curve geometries. The main additional degrees of freedom available, as compared to Hilbert or Peano curves, can be summarized as follows:

- *Arbitrary* choice of endpoints (see, the examples in Fig. 1).
- Possibility of dealing with *non-Cartesian* grids and *non-rectangular* footprints. For instance, Figure 2 shows some examples of HP realizations in a triangular grid with triangular [Fig. 2(a)] and hexagonal [Fig. 2(b)] footprint, and in a hexagonal lattice with hexagonal footprint [Fig. 2(c)].
- Possibility of generating *constrained* realizations. For instance, Figure 3 shows some HP realizations in a 16×16 GG, generated via the cost-based TSP approach in Section 2.2 by constraining part of the curve (solid line) to coincide with a 4th-iteration Hilbert curve, while leaving the remaining part (dashed line) unconstrained.

3. METAMATERIAL INCLUSIONS BASED ON GRID-GRAPH HAMILTONIAN PATHS

With a view toward exploring possible applications of GG-HP-based metamaterial inclusions we began studying the plane-wave scattering from electrically small loops corresponding to 6×6 GG-HC. In this case, the relatively small number of possible realizations (1072) ensures the computational viability of a comprehensive *full-wave* study. In our simulations, the perfectly-electric-conducting (PEC) loops were assumed to be placed in the x-y plane, and to be illuminated by a normally-incident plane-wave with y-polarized unit-amplitude electric field and $\exp(j\omega t)$ time-harmonic dependence. It is worth highlighting that, by construction, all the HC realizations occupy the same square footprint of side length L_S, and exhibit the same total length $L_{HC} = 36L_S/5$ and internal area $A_{HC} = 17L_S^2/25$. Therefore, possible differences in the EM responses should be attributed to the actual geometric structure. To solve the plane-wave scattering problem, we used a moment-method-based [NEC-2 (http://www.nec2.org)] engine. From the current distribution on the wire, computed for each HC realization at many frequencies, we first analyzed the (lowest) resonant frequency, corresponding (as in Ref. 7, 8) to the maximum value of the (peak) current on the loop. The statistical distribution of the resonant frequencies, not shown here for brevity, turned out to be *nearly uniform* within an interval of $\pm 10\%$ around an average value corresponding to a total electrical length of 1.12 wavelengths. In this connection, we also observed some loose correlation between the resonant frequencies and a geometrical metric (defined as the ratio between the number of right angles in the HC and the total number of vertices) accounting for the "curliness" of the HC, which deserves further in-depth investigation. Next, we considered the electric far-field in the standard (r,θ,ϕ) spherical coordinate system:

$$\boldsymbol{E}(\theta,\phi) = -j\eta_0 \frac{\exp(-jk_0 r)}{2\lambda_0 r}[\boldsymbol{N} - \hat{u}_r \boldsymbol{N}(\theta,\phi)\cdot\hat{u}_r], \qquad (1)$$

where $\eta_0 = \sqrt{\mu_0/\varepsilon_0}$ denotes the free-space characteristic impedance, $k_0 = \omega\sqrt{\varepsilon_0\mu_0} = 2\pi/\lambda_0$ denotes the free-space wavenumber (with λ_0 denoting the wavelength), and $\boldsymbol{N}(\theta,\phi)$ is the radiation vector. In Eq. (1), and henceforth, $\hat{u}_a$ denotes an α-directed unit vector. For small loops, the following approximate multipole parameterization [26] can be used for the radiation vector in Eq. (1):

$$\boldsymbol{N}(\theta,\phi) = \boldsymbol{N}^{(p)}(\theta,\phi) + \boldsymbol{N}^{(m)}(\theta,\phi) + \boldsymbol{N}^{(Q)}(\theta,\phi) = j\omega\boldsymbol{p} + jk_0\boldsymbol{m}\times\hat{u}_r - \omega k_0 \underline{\underline{Q}}\cdot\hat{u}_r. \qquad (2)$$

In Eq. (2), $\boldsymbol{p}$ and $\boldsymbol{m}$ denote the electric and magnetic dipole moments, respectively,

$$p = \frac{1}{j\omega}\int_{HC} I(s)d\boldsymbol{r}(s), \quad \boldsymbol{m} = \frac{1}{2}\int_{HC} I(s)\boldsymbol{r}(s)\times d\boldsymbol{r}(s), \qquad (3)$$

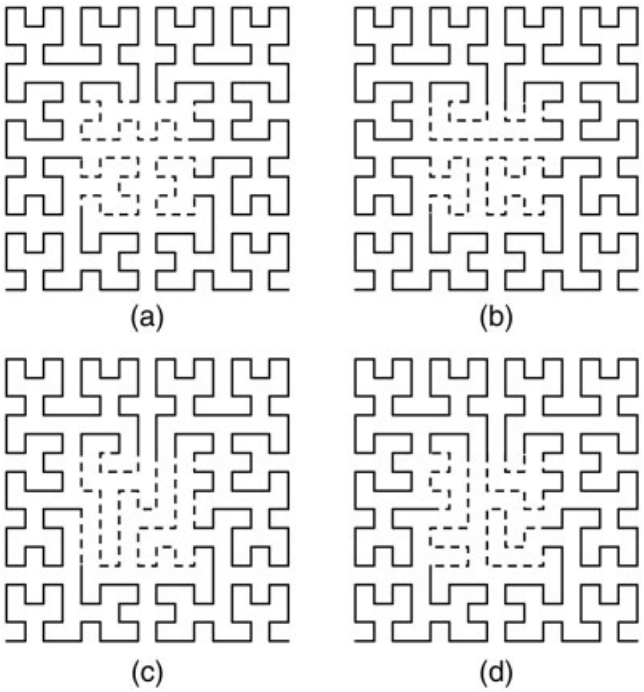

Figure 3 Examples of *constrained* HP realizations in a 16×16 GG. The continuous-line part is constrained to a 4th-iteration Hilbert curve, whereas the dashed-line part is free. (a) Hilbert; (b)–(d) Other realizations

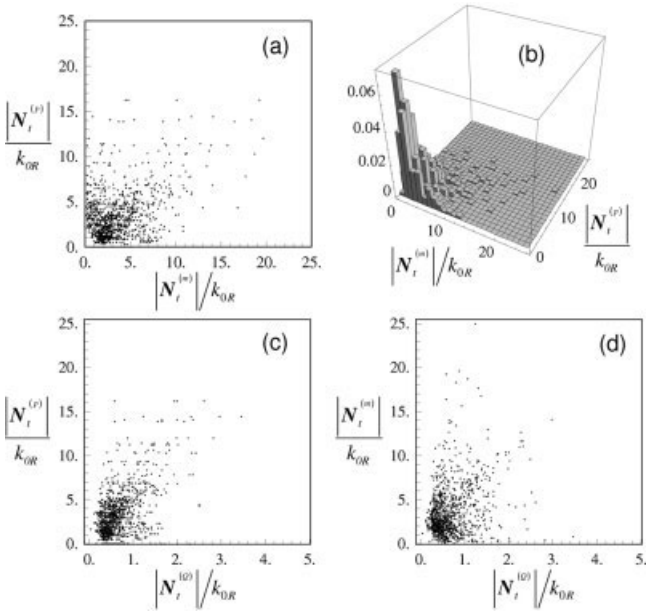

Figure 4 Two-fold joint distributions, computed over the 1072 HC realizations in a 6×6 GG, of the multipole constituents in the (transverse) radiation vector (maximum over θ,ϕ, at resonance) in Eq. (2), scaled to resonant wavenumber k_{0R}. A normally-incident plane-wave illumination is assumed, with unit-amplitude y-polarized electric field; PEC HC elements are assumed to occupy a square footprint in the x-y plane (with side-length L_S, total wire-length $L_{HC} = 36L_s/5$, and wire radius $= 1.7 \cdot 10^{-4}L_s$). (a), (b) Scatter plot and joint-distribution histogram, respectively, pertaining to $N_t^{(p)}$ vs. $N_t^{(m)}$; (c), (d) Scatter plots pertaining to $N_t^{(p)}$ and $N_t^{(m)}$, respectively, vs. $N_t^{(Q)}$

with $I(s)$ denoting the current distribution on the loop, whereas $\underline{\underline{Q}}$ denotes the electric quadrupole dyadic, with Cartesian components $(\alpha,\beta = x,y,z)$:

$$Q_{\alpha\beta} = \frac{1}{2j\omega}\int_{HC} I(s)[\alpha(s)\hat{u}_t(s)\cdot\hat{u}_\beta + \beta(s)\hat{u}_t(s)\cdot\hat{u}_\alpha]ds. \qquad (4)$$

Figure 4 shows the two-fold joint distributions of the various multipole constituents in the (transverse) radiation vector (maximum over θ,ϕ, at resonance), computed over the 1072 HC realizations. Specifically, the scatter plot in Figure 4(a) pertains to the $N_t^{(p)}$ ("electric dipole") vs. $N_t^{(m)}$ ("magnetic dipole") responses, and visually reveals the wealth of EM responses that can be obtained as the sole effect of geometry. Although most of the response samples tend to be clustered around the smaller strength values, as more clearly visible from the joint-distribution histogram in Figure 4(b), there are a considerable number of outliers with response strengths spanning a significant range. In particular, one can identify HC geometries with predominant *electric* or *magnetic* dipole responses, and others for which the two response strengths are comparable (and thus, in view of Eqs. (2) and (3), are potentially capable of supporting circular polarization). Figures 4(c) and 4(d) show the scatter plots pertaining to the electric and magnetic dipole responses, respectively, vs. the electric quadrupole response $(N_t^{(Q)})$. It is observed that the spread in the quadrupole response strength is significantly smaller. We searched for possible HC realizations exhibiting a predominant *quadrupole* response (similar to what recently observed in spherical inclusions with properly-tuned metamaterial coatings [27]), but were not able to identify any particularly interesting configuration in this respect.

The implications of the above preliminary results in the synthesis of HP-based inclusions for single- and double-negative metamaterials are currently under investigation. In what follows, we focus on possible applications to *artificial magnetic conductors* (AMC). In this connection, previous studies on configurations based on frequency-selective surfaces composed of periodic arrangements of Hilbert [7] and Peano [8] curve inclusions closely located above a PEC ground plane have highlighted potential advantages and limitations. In particular, these configurations seem to suffer from a significant dependence on the incident-field polarization, which can be mitigated by utilizing macro-cells composed of Hilbert/Peano-curves in different orientations [28]. Against this background, we searched for possible 6×6 GG-HC realizations exhibiting *reduced polarization-sensitivity*. Figure 5 illustrates the results pertaining to a particularly interesting candidate geometry (displayed in the inset), computed using a moment-method-based commercial software [IE3D version 9.35 (http://www.zeland.com/ie3d.html)]. Specifically, Figure 5(a) shows the radar-cross-section (RCS) response of a single PEC inclusion in free space, for normally-incident plane-wave illumination with two orthogonal (x,y) polarizations. A fairly weak dependence on the incident field polarization is observed. Figure 5(b) shows the reflection coefficient (Γ) phase, for orthogonal plane-wave incidence, of an infinite two-dimensional periodic array of such elements closely located above a conducting ground-plane (with parameters detailed in the figure caption). As expected, a typical AMC behavior (null phase) is observed, nearly independent of the field polarization.

This serves as an illustration of the possible design improvements attainable through a judicious exploitation of the inherent flexibility of HP geometries. Possible practical applications of the above results are envisaged in the design of polarization-independent thin radar absorbers for RCS reduction, and ground-planes for low-profile/printed dual-polarized antennas (for polarization diversity) or circularly-polarized antennas (for improving the axial-ratio near the horizon).

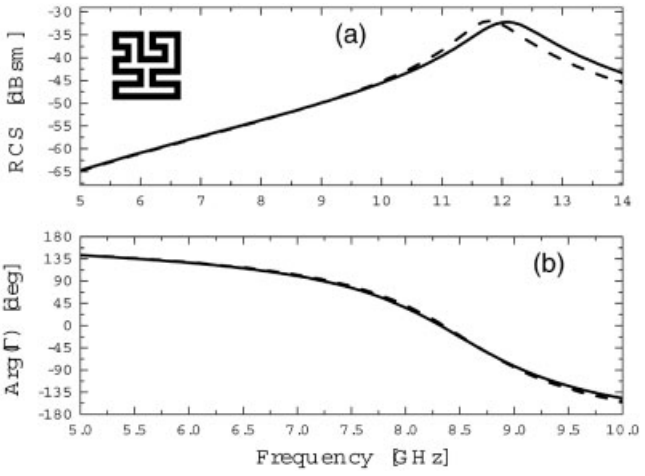

Figure 5 Application to reduced-polarization-sensitivity AMC. (a) RCS response of a single PEC HC element in free space, with geometry as in the inset (5×5 mm^2 footprint, 0.5 mm-wide strip), for normally-incident plane-wave illumination. (b) Reflection-coefficient phase of an infinite two-dimensional array of same HC elements (with 1 mm inter-element spacing) placed 2.5 mm above a PEC ground plane. Continuous line: y-polarized electric field; Dashed line: x-polarized electric field

4. CONCLUSIONS AND PERSPECTIVES

In this article, we have explored the EM properties of a fairly broad class of space-filling curve geometries (which includes as special cases the well-known Hilbert and Peano curves) based on the concept of GG-HP. After a compact overview of the GG-HP background theory and generation algorithms, we have focused on possible applications to metamaterial loop-type inclusions. As an illustration of the HP-framework potentials, we have presented an application example involving AMC with reduced polarization-sensitivity.

Current and future research are aimed at better understanding the role of geometry, through comprehensive parametric analysis, and possible correlation of the EM response with geometrical-complexity (e.g., entropy-based) metrics. Also worth of interest, from the application viewpoint, is the development of strategies (based, e.g., on evolutionary optimization) for systematic exploitation of inherent flexibility of HP geometries, as well as further studies of HP-based metamaterial inclusions, miniaturized and/or self-structuring antennas, and RFID encoding strategies.

REFERENCES

1. H. Sagan, Space-filling curves, Springer-Verlag, Berlin, 1994.
2. K.J. Vinoy, K.A. Jose, V.K. Varadan, and V.V. Varadan, Hilbert curve fractal antenna: A small resonant antenna for VHF/UHF applications, Microwave Opt Technol Lett 29 (2001), 215–219.
3. J. Anguera, C. Puente, E. Martínez, and E. Rozan, The fractal Hilbert monopole: A two-dimensional wire, Microwave Opt Technol Lett 36 (2003), 102–104.
4. J. Zhu, A. Hoorfar, and N. Engheta, Bandwidth, cross-polarization, and feed-point characteristics of matched Hilbert antennas, IEEE Antennas Wireless Propag Lett 2 (2003), 2–5.
5. J. Zhu, A. Hoorfar, and N. Engheta, Peano antennas, IEEE Antennas Wireless Propag Lett 3 (2004), 71–74.
6. E.A. Parker and A.N.A. El Sheikh, Convoluted array elements and reduced size unit cells for frequency-selective surfaces, IEE Proc H: Microwave Antennas Propag 138 (1991), 19–22.
7. J. McVay, N. Engheta, and A. Hoorfar, High impedance metamaterial surfaces using Hilbert-curve inclusions, IEEE Microwave Wireless Components Lett 14 (2004), 130–132.
8. J. McVay, A. Hoorfar, and N. Engheta, Peano high-impedance surfaces, Radio Sci 40 (2005), RS6S03.
9. J. McVay, N. Engheta, and A. Hoorfar, Numerical study and parameter estimation for double-negative metamaterials with Hilbert-curve inclusions, In: Proceedings of 2005 IEEE Antennas Propagation Society International Symposium, Washington, DC, July 3–8, 2005, vol. 2B, pp. 328–331.
10. J. McVay, A. Hoorfar, and N. Engheta, Space-filling curve RFID tags, In: Proceedings of IEEE Radio and Wireless Symposium, San Diego, CA, Jan. 17–19, 2006, pp. 199–202.
11. S.R. Best and J.D. Morrow, The effectiveness of space-filling fractal geometry in lowering resonant frequency, IEEE Antennas Wireless Propag Lett 1 (2002), 112–115.
12. S.R. Best, A comparison of the resonant properties of small space-filling fractal antennas, IEEE Antennas Wireless Propag Lett 2 (2003), 197–200.
13. S.R. Best, A discussion on the significance of geometry in determining the resonant behavior of fractal and other non-Euclidean wire antennas, IEEE Antennas Propag Mag 45 (2003), 9–28.
14. J.M. Gonzalez-Arbesu, S. Blanch, and J. Romeu, Are space-filling curves efficient small antennas? IEEE Antennas Wireless Propag Lett 2 (2003), 147–150.
15. S.R. Best, A comparison of the performance properties of the Hilbert curve fractal and meander line monopole antennas, Microwave Opt Technol Lett 35 (2002), 258–262.
16. V. Pierro, V. Galdi, I.M. Pinto, J. McVay, N. Engheta, and A. Hoorfar, Electromagnetic properties of space-filling wire structures based on grid-graph Hamiltonian paths: Some preliminary results, In: Proceedings of 2005 URSI National Radio Science Meeting, Washington, DC, July 3–8, 2005, p. 214.
17. J.A. Bondy and U.S.R. Murty, Graph theory with applications, Elsevier, Amsterdam, 1976.
18. O. Ore, A note on Hamiltonian circuits, Am Math Mon 67 (1960), 55.
19. A. Itai, C.H. Papadimitriou, and J. Szwarcfiter, Hamilton paths in grid graphs, SIAM J Comput 11 (1982), 676–686.
20. R.E. Miller and J.W. Thatcher (Eds.), Complexity of computer computations, Plenum Press, New York, 1972.
21. R. Stoyan and V. Strehl, Enumeration of Hamiltonian circuits in rectangular grids, J Combin Math Combin Comput 21 (1996), 109–127.
22. S. Martello, An enumerative algorithm for finding Hamiltonian circuits in a directed graph, ACM Trans Math Software 9 (1983), 131–138.
23. W. Kocay, An extension of the multi-path algorithm for finding Hamilton cycles, Discrete Math 101 (1992), 171–188.
24. D. Angluin and L.G. Valiant, Fast probabilistic algorithms for Hamiltonian circuits and matchings, J Comput Syst Sci 18 (1979), 155–193.
25. E. Lawler, J. Lenstra, A. Rinnooy Kan, and D. Shmoys, The traveling salesman problem: A guided tour of combinatorial optimization, Wiley, New York, 1985.
26. C.H. Papas, Theory of electromagnetic wave propagation, Dover, New York, 1988.
27. A. Alù and N. Engheta, Polarizabilities and effective parameters for collections of spherical nanoparticles formed by pairs of concentric double-negative, single-negative, and/or double-positive metamaterial layers, J Appl Phys 97 (2005), 094310.
28. J. McVay, A. Hoorfar, and N. Engheta, Bandwidth enhancement and polarization dependence reduction for space-filling curve artificial magnetic conductors, Presented at 2005 URSI Nat Radio Sci Meeting, Washington, DC, July 3–8, 2005.

FURTHER COMMENTS ON THE PERFORMANCES OF FINITE ELEMENT SIMULATORS FOR THE SOLUTION OF ELECTROMAGNETIC PROBLEMS INVOLVING METAMATERIALS

Gaia Cevini,[1] Giacomo Oliveri,[2] and Mirco Raffetto[2]
[1] Department of Electronics
University of Pavia
Italy
[2] Department of Biophysical and Electronic Engineering
University of Genoa
Italy

Received 29 May 2006

ABSTRACT: *In this paper, we analyze the performances of three-dimensional finite element (FE) simulators in handling electromagnetic scattering problems involving metamaterials. It has already been proved that the performances of the FE method are worse than usual, when metamaterials are considered. In this work, we extend our previous analysis by providing some additional results on the precision of the FE solution and on the performances of the iterative and direct solvers typically used with FE simulators.* © 2006 Wiley Periodicals, Inc.
Microwave Opt Technol Lett 48: 2524–2529, 2006; Published online in Wiley InterScience (www.interscience.wiley.com). DOI 10.1002/mop.22008

Key words: *metamaterials; finite element method; electromagnetic scattering; performances of finite element simulators*